Materials Science Forum Vol. 758 (2013) pp 147-156

doi:10.4028/www.scientific.net/MSF.758.147

Shape Memory Alloy Helical Springs Performance: Modeling and Experimental Analysis

Ricardo Alexandre Amar de Aguiar[1,a],

Waldyr Cardoso de Castro Leão Neto[1,b], Marcelo Amorim Savi[2,c]
and Pedro Manuel Calas Lopes Pacheco[1,d]

[1]CEFET/RJ, Centro Federal de Educação Tecnológica Celso Suckow da Fonseca, Department of Mechanical Engineering, 20.271.110, Rio de Janeiro, RJ, Brazil

[2]COPPE/UFRJ, Department of Mechanical Engineering, Caixa postal 68.503, Rio de Janeiro, RJ, 21941-972, Brazil

[a]raaguiar@cefet-rj.br, [b]waldyrleao@yahoo.com.br, [c]savi@mecanica.ufrj.br, [d]calas@cefet-rj.br

Keywords: Shape Memory Alloy; Modeling; Experimental Analysis; Helical Spring

Abstract. Shape memory alloys (SMAs) are metallic materials that have the capability to recover its original shape eliminating residual strains when subjected to adequate thermal process. This behavior is related to phase transformation induced either by stress or by. During the phase transformation process of an SMA component, large loads and/or displacements can be generated in a relatively short period of time making this component an interesting mechanical actuator. Because of such remarkable properties, SMAs have found a number of applications in different areas. The present contribution deals with the modeling, simulation and experimental analysis of SMA helical springs. Basically, it is assumed a one-dimensional constitutive model to describe its thermomechanical shear behavior and, afterwards, helical springs are modeled by considering classical approach. SMA helical spring thermomechanical behavior is investigated through experimental tests performed at different loads. Numerical results show that the model is in close agreement with experimental data. Since the thermal process has an essential importance in the performance of an SMA actuator, different cooling medium conditions are investigated, evaluating the actuators performance.

Introduction

Shape memory alloys (SMAs) present complex thermomechanical behaviors related to different physical processes. The most common phenomena presented by this class of material are the pseudoelasticity, the shape memory effect, which may be one-way (SME) or two-way (TWSME), and the phase transformation due to temperature variation. Besides these phenomena, there are more complicated effects that have significant influence over its overall thermomechanical behavior – for instance: plastic behavior, tension-compression asymmetry, plastic-phase transformation coupling, transformation induced plasticity, thermomechanical coupling, among others [1,2]. The remarkable properties of SMAs are attracting much technological interest, motivating different applications in several fields of sciences and engineering. Aerospace, biomedical, and robotics are some areas where SMAs have been applied [3-15]

SMAs have the capability to generate large strains associated with phase transformation induced by stress and/or temperature variations [16]. During the phase transformation process of an SMA component, large loads and/or displacements can be generated in a relatively short period of time making this component an interesting mechanical actuator. Basically, SMA presents two possible phases: martensite and austenite. Martensitic phase may appear in variants induced by different kinds of stress fields [17,18]. Several alloys can develop strains associated with phase transformation but only those that can develop large strains have commercial interest, as nickel-titanium (NiTi) and copper base alloys (CuZnAl and CuAlNi).

The complex thermomechanical behavior of SMAs makes their modeling a difficult task. This may introduce difficulties in the evaluation of SMA applications. SMA springs are an important actuator that can be used in different kinds of application. There are some efforts to model the SMA helical springs thermomechanical behavior [19-21]. In the present contribution, Brinson's constitutive model, originally proposed for one-dimensional tensile-compressive behavior, is employed to describe the shear behavior. Afterward, it is developed an SMA helical spring model by assuming that the spring wire presents a homogeneous phase transformation. Besides, an experimental apparatus is employed to evaluate the thermomechanical behavior of the spring. Numerical and experimental results are compared evaluating different thermomechanical loadings. Since the thermal process has an essential importance in the performance of an SMA actuator, different cooling medium conditions are investigated. In this regard, thermomechanical coupling effects are investigated for different environments.

Constitutive Model

SMA thermomechanical behavior can be described by different constitutive models. Paiva [22] presented an overview of constitutive models for SMAs. Here, the model with assumed transformation kinetics proposed by Brinson [23] is employed. This one-dimensional model assumes a prescribed function for the phase transformation kinetics establishing a relationship between the martensitic volume fraction, β, with temperature, T, and one-dimensional strain, ε. Brinson's model considers that martensitic volume fraction is composed by two distinct parts: temperature induced martensitic fraction, β_T, and stress-induced martensitic fraction, β_S. Therefore $\beta = \beta_T + \beta_S$.

Although this one-dimensional constitutive model is originally proposed to describe tension-compression behavior, it has been noted that experimental torsion test curves presented in different references [24, 25] indicate that these curves are qualitatively similar to those obtained in tension tests performed in Ni-Ti and other SMAs. Based on this observation, this constitutive model is employed to describe the pure shear stress state, replacing the stress, strain, and elastic modulus, respectively, by the shear stress, τ, shear strain, γ, and shear modulus, G. Under this assumption, it is possible to obtain a complete set of constitutive equations that describes the thermomechanical behavior of SMAs. The shear stress evolution is represented by the following equation:

$$\dot{\tau} = G\dot{\gamma} + \alpha\dot{\beta}_S \tag{1}$$

where $G = G_M + \beta\,(G_A - G_M)$ is the shear modulus and α is a coefficient associated with phase transformation. G_A is the austenite shear modulus and G_M is the martensite shear modulus.

The phase transformation is determined by the current values of stress and temperature, $\beta = \beta(\tau, T)$. For $T > M_S$ the transformation from austenite to detwined martensite is described by:

$$\beta_S = \frac{1-\beta_S}{2}\cos\left\{\left(\frac{\pi}{\tau_S^{CRIT} - \tau_f^{CRIT}}\right)\left[\tau - \tau_f^{CRIT} - C_M(T - M_S)\right]\right\} + \frac{1+\beta_{S0}}{2} \tag{2}$$

$$\beta_T = \beta_{T0} - \frac{\beta_{T0}}{1-\beta_{S0}}(\beta_S - \beta_{S0}) \tag{3}$$

where τ_S^{CRIT} and τ_f^{CRIT} are critical stress for martensitic transformation start and finish, C_M is a positive constant and β_{T0} and β_{S0} represents the volume fractions of martensite before transformation begins to take place. This equation holds for $\tau_S^{CRIT} + C_M(T - M_S) < \tau < \tau_f^{CRIT} + C_M(T - M_S)$. For $T < M_S$ and $\tau_S^{CRIT} < \tau < \tau_f^{CRIT}$:

$$\beta_S = \frac{1-\beta_{S0}}{2}\cos\left[\frac{\pi}{\tau_S^{CRIT}-\tau_f^{CRIT}}(\tau-\tau_f^{CRIT})\right]+\frac{1+\beta_{S0}}{2} \quad ; \quad \beta_T = \beta_{T0}-\frac{\beta_{T0}}{1-\beta_{S0}}(\beta_S-\beta_{S0})+\Delta T \tag{4}$$

$$\text{where } \Delta T = \begin{cases} \left\{\frac{1-\beta_T}{2}\left\{\cos\left[\frac{\pi}{M_S-M_F}(T-M_f)\right]+1\right\}\right. & \text{for } M_F < T < M_S, T < T_0 \\ 0 & \text{otherwise} \end{cases}$$

The reverse transformation occurs for $T > A_S$ and $C_A(T-A_F) < \tau < C_A(T-A_S)$, where C_A is a positive constant, and is described by:

$$\beta_S = \frac{\beta_S}{2}\left\{\cos\left[\frac{\pi}{A_f-A_S}(T-A_S-\frac{\tau}{C_A}\right]+1\right\} \quad ; \quad \beta_T = \frac{\beta_{T0}}{2}\left\{\cos\left[\frac{\pi}{A_f-A_S}(T-A_S-\frac{\tau}{C_A}\right]+1\right\} \tag{5}$$

Shape Memory Alloy Helical Spring

The modeling of the restoring force produced by a shape memory alloy spring is done considering a helical spring with diameter *D*, built with *N* coils with a wire diameter *d*. It is assumed that the longitudinal force, *F*, is resisted by the torsional shear stress developed on the circular cross section of the helical shaped wire (Fig. 1).

Figure 1. Helical spring [26].

$$F = \frac{4\pi}{D}\int_0^{d/2}\tau\, r^2 dr \tag{6}$$

where *r* is the radial coordinate along the wire cross section. It is also assumed that the shear strain is linearly distributed along the wire cross section, from what follows the kinematics relation

$$\gamma = \frac{d}{\pi D^2 N}u \tag{7}$$

where *u* is the spring displacement.

The force-displacement relation is obtained by assuming that the wire presents a homogeneous phase transformation through the wire cross-section. Therefore, the integration results in the following expression:

$$F = \frac{\pi d^3}{6D}\left(\frac{Gd}{\pi D^2 N}u - \alpha\beta\right) \tag{8}$$

This equation together with those that describes the volume fraction evolution establishes a proper description of the thermomechanical behavior of SMA helical springs.

Besides, the energy balance for the SMA spring may be written considering a lumped formulation:

$$\rho r - \frac{hA}{L}(T-T_\infty) = c\rho\dot{T} \tag{9}$$

where ρ is the density, L the helical spring total wire length, r a heat source, h the convection coefficient, A the convection surface area, T_∞ the medium temperature and c the specific heat. Temperature variations can be induced in the SMA helical spring through joule effect by the application of an electrical current. Therefore $r = RI^2$, where R is the SMA linear electric resistance and I is the applied electric current.

Experimental Procedure

An experimental apparatus, shown in Fig. 2, is employed to investigate the thermomechanical behavior of SMA helical springs. This set up is composed of a rigid frame that has a load cell (Alfa SV-20 with 196 N capacity) fixed at the top. The SMA spring is connected to the load cell and the other end is attached to a dead load. A laser sensor is employed to monitor displacements (Micro-Epsilon ILD 2220-100). Temperature variations are induced through joule effect by the application of an electrical current using a stabilized current source (Minipa MPL-1303). The spring temperature is monitored by an infrared camera (FLIR A-320).

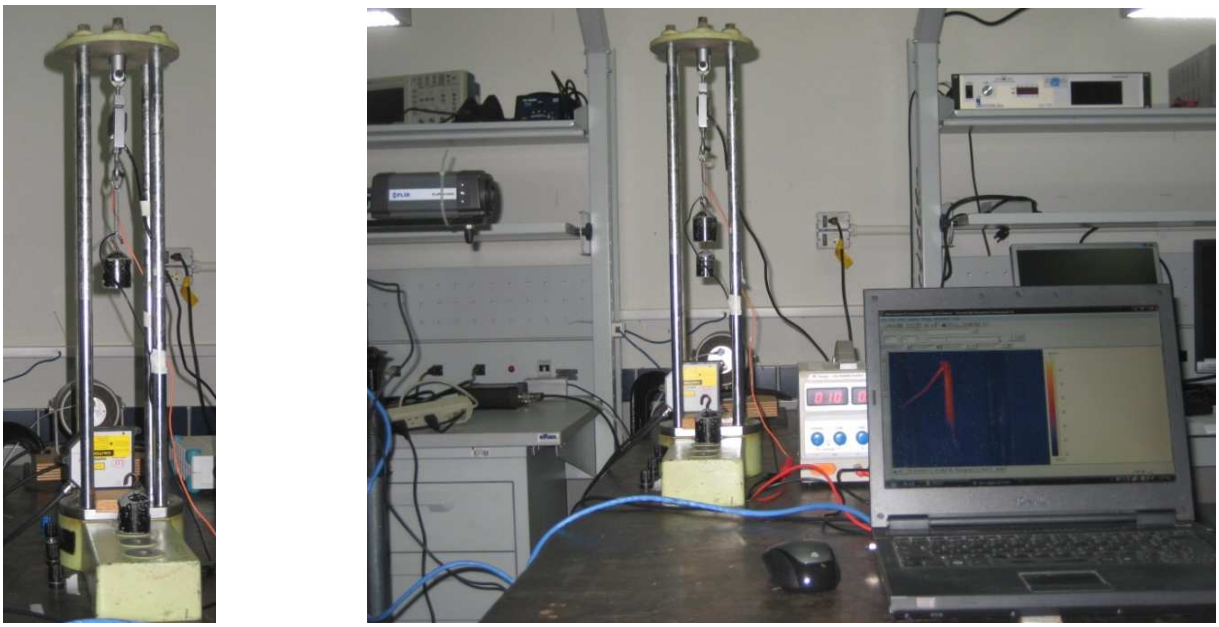

(a) (b)

Figure 2. Experimental apparatus: (a) Rigid frame; (b) Thermal infrared image of the SMA spring subjected to an electronic current

The thermomechanical tests have by three stages: 1) mechanical loading, 2) thermal heating and 3) thermal cooling. In the first one, a constant load (dead load) is attached to the SMA spring free end until a static equilibrium state is reached. Three different levels of loads are considered: 2.3, 3.3 and 4.1 N. For the thermal heating, SMA helical spring temperature is raised above A_F by applying an electrical current: of 1.5, 2.0 and 2.5 A. All tests are performed at room temperature (20ºC). Finally, the thermal cooling stage consists of SMA spring cooling through convection with the surrounding medium.

An SMA NiTi spring with an external diameter of 6 mm, a wire diameter of 0.75 mm and 20 active coils is used. Aguiar [27] presented a thermomechanical characterization of SMA springs. Here the characterization is performed from experimental results obtained from displacement-current (Fig. 3a), DSC (Fig. 3b) and displacement time evolution (Fig. 4) tests, defining important aspects related to the SMA phase transformations. Figs. 4a-4c shows that the applied electric current levels are enough to promote the complete spring recovery and, as expected, larger values promote faster responses in the heating stage. Fig. 4*d* shows that recovered displacement of 17, 27 and 50 mm are obtained during heating stage for loads of 2.3, 3.3 and 4.1 N, respectively.

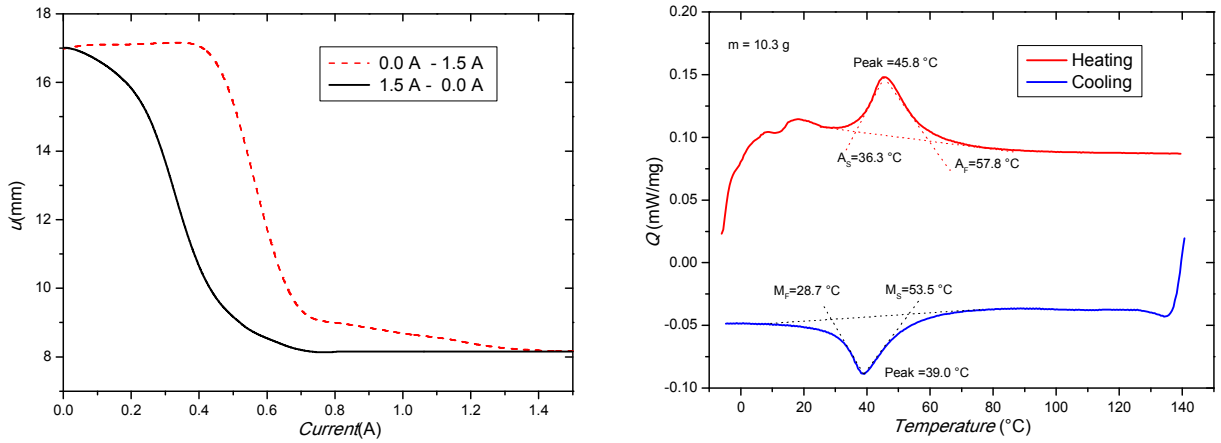

(*a*) (*b*)

Figure 3. Experimental data: (a) Displacement-electric current curves; (b) DSC analysis.

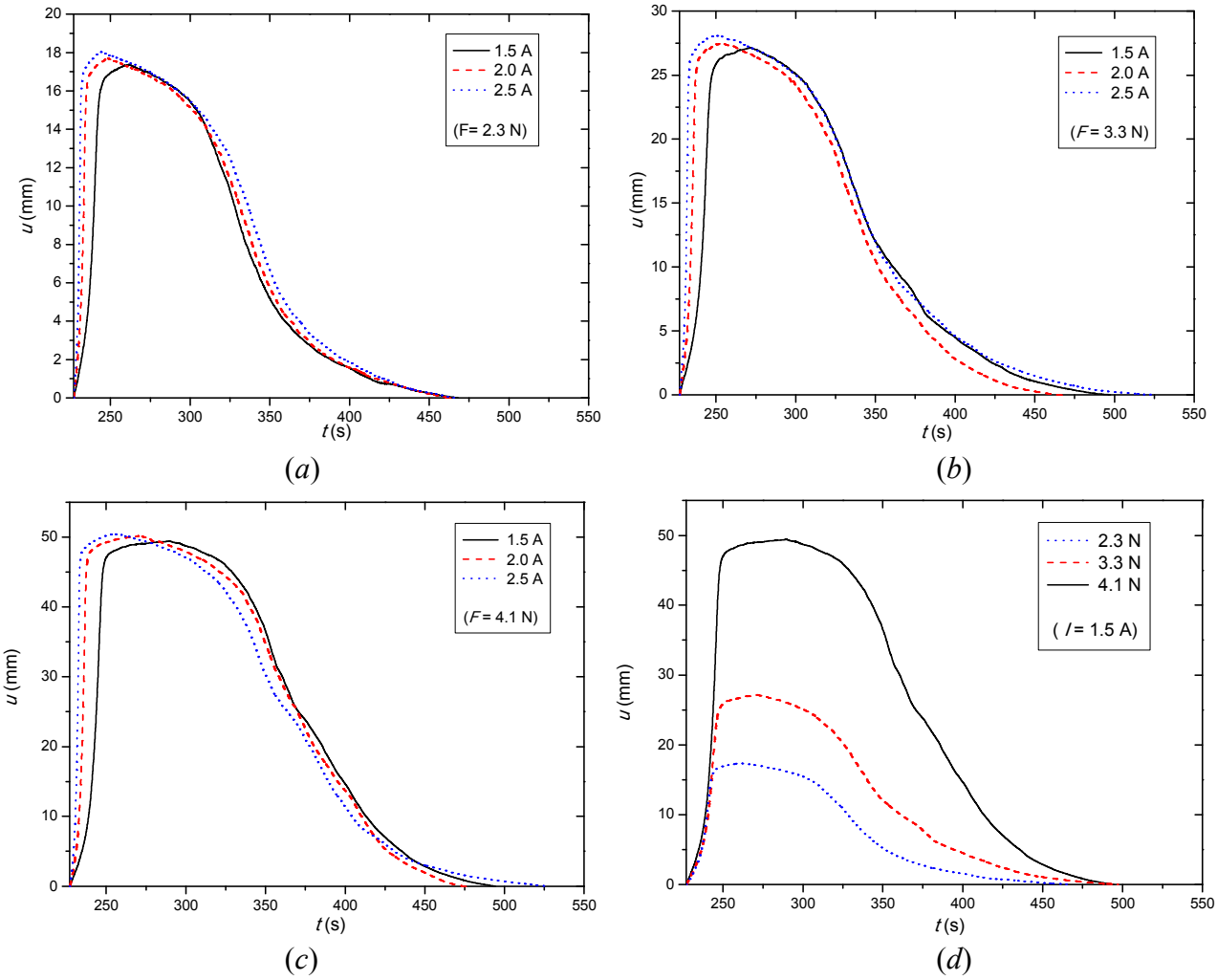

(*a*) (*b*) (*c*) (*d*)

Figure 4. Experimental data related to the spring mechanical loading a thermal heating-cooling displacement. Effect of the electric current for 3 load levels: (a) 2.3 N (b) 3.3 N and (c) 4.1 N. (d) Effect of the load for electric current of 1.5 A.

Numerical Simulations

The numerical procedure adopted is based on the operator split technique [28] associated with an iterative scheme in order to deal with nonlinearities in the formulation. Under this assumption, coupled governing equations are solved from three uncoupled problems: thermal, mechanical and phase transformation behaviors. Therefore, the following moduli are considered:

Thermal Problem - Comprises a transient thermal lumped model with a heat source (joule effect) and surface convection. Energy (Eq. 9) is integrated using a simple Euler method.

Mechanical Problem - Stress and displacement are evaluated from temperature evolution using Eq. 1, Eq.7, Eq. 8 and a prescribed force.

Phase Transformation Problem - The volume fractions of the phases are determined using Eq. 2, Eq.3, Eq.4 and Eq.5.

Initially, numerical simulations are carried out establishing a comparison with experimental data presented in the previous section. Model parameters are estimated in order to match experimental tests, being presented in Table 1.

Table 1. SMA model parameters.

Parameter	Value
G_M (GPa)	11.5
G_A (GPa)	14.5
α (MPa)	220
τ_S^{crit} (MPa)	57.7
τ_F^{crit} (MPa)	98.2
C_M (MPa)	3.6
C_A (MPa)	13

Parameter	Value
M_f (ºC)	29
M_s (ºC)	42
A_s (ºC)	43
A_f (ºC)	58
ρ (Kg/m^3)	6453
c (J/Kg K))	465
R (Ω/m)	2
h (W/m^2 C)	2

Fig. 5*a* shows a comparison between experimental and numerical data for a load of 4.1 N considering an electric current of 1.5 A. A good agreement is noticeable. Besides this result, Fig. 5*b* shows the shear stress-strain curve while Fig. 6 shows the temperature and phase transformation time evolution. Results represent the general thermomechanical behavior of SMAs, strongly related to phase transformations.

The actuation capacity of an SMA is associated with the amount of stress-induced martensite during mechanical loading stage. This is represented by volume fraction, being related to residual strain/displacement, which can be eliminated during heating stage. The major drawback about the use of SMAs as actuators may be the slow cooling period that depends directly on the heating and cooling time. During the cooling stage heat must be removed from the SMA actuator and usually, this is done by convection through a cooling medium as air or a cooling fluid. Therefore, it is important to investigate thermal characteristics of the process associated with different cooling medium and conditions. Seven different convection coefficients are considered: 0.5, 1, 2, 4, 8, 16 and 32 W/m^2 °C. The electric current is adjusted to promote a maximum temperature value approximately 70 °C during the heating stage. An electric current of 1.5 A is adopted except for h = 32 W/m^2 °C, where 1.7 A is considered. Fig. 7 shows the displacement and temperature evolution for these conditions. This picture shows that the actuation times are strongly dependent of the convection coefficient of the medium varying from 820 s to 15 s.

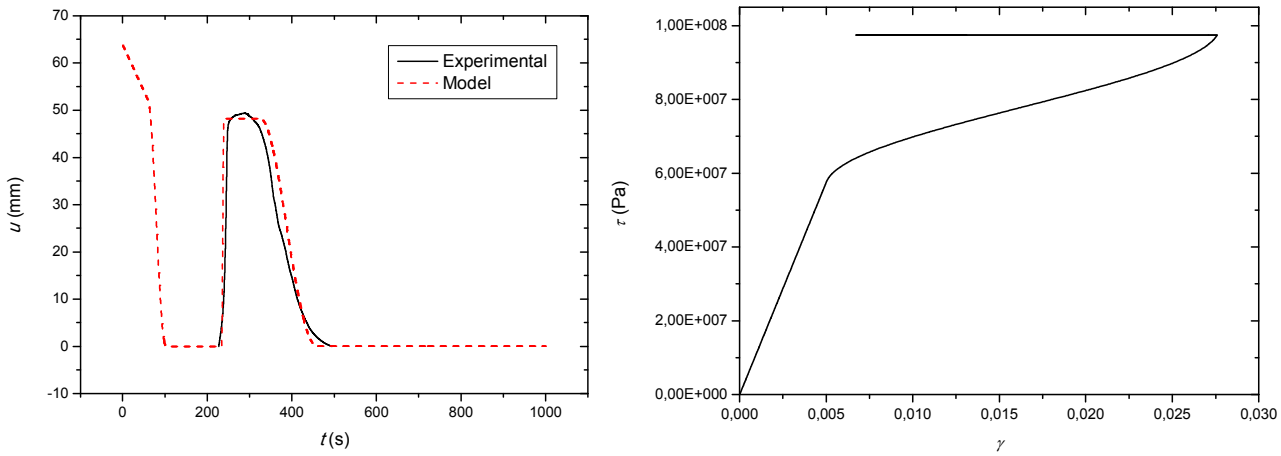

Figure 5. Numerical and experimental comparison: (*a*) displacement evolution. (*b*) shear stress-strain curve. F = 4.1 N and I= 1.5 A.

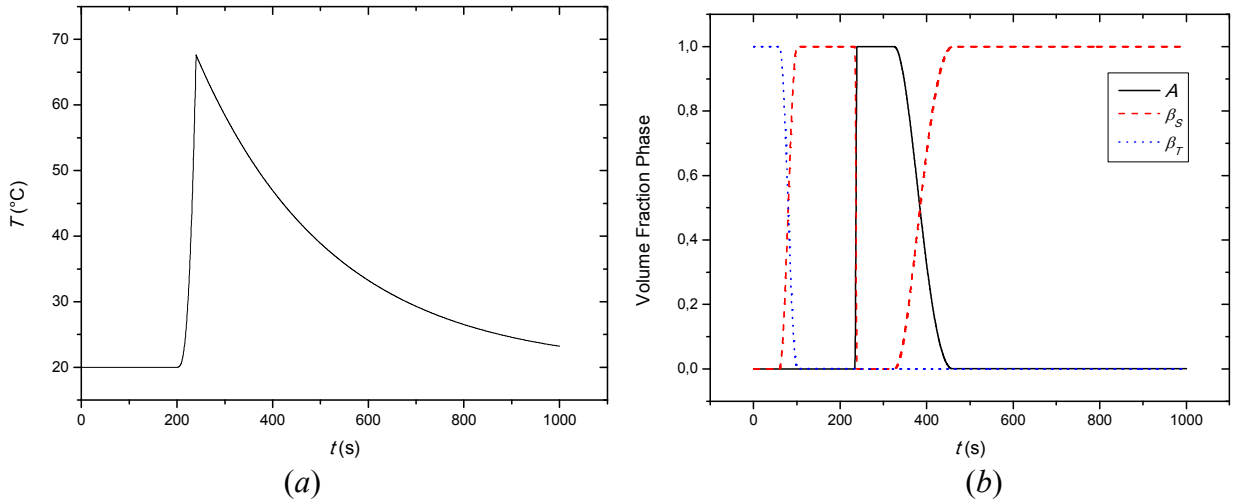

Figure 6. (a) Temperature and (*b*) phase transformation evolution. F = 4.1 N and I = 1.5 A.

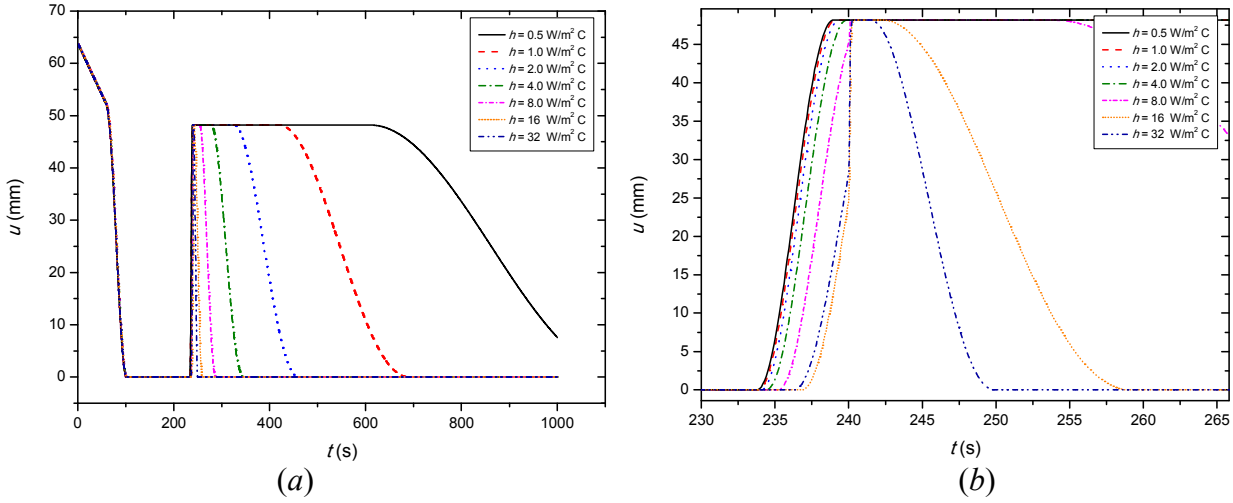

Figure 7. (a) Displacement evolution for several convection coefficients and (b) a zoon in the heating stage. F = 4.1 N and I = 1.5 A (except for h =32 W/m^2 C where I = 1.7 A).

Table 2 and Fig. 8 present data associated with the performance of the SMA device as a function of convection coefficient. These results indicate that actuation time can be the major drawback of SMA actuators that uses convection as the heat removal mechanisms. Nevertheless, the

performance can be improved with solutions using forced convection, special fluids with high capability of heat removal or mechanisms based on the Peltier-effect thermoelectric devices for selective local heating and cooling [29-31].

Table 2. Performance of SMA helical springs actuators.

	h (W/m^2°C)						
	0.5	**1**	**2**	**4**	**8**	**16**	**32**
Actuation Time (s)	820	445	220	110	50	25	15
Heating velocity (mm/s)	9.8	9.4	9.1	8.5	7.6	7.6	7.6
Cooling velocity (mm/s)	0.1	0.2	0.4	0.8	1.6	5.0	6.3
Actuation Frequency (Hz)	0.001	0.002	0.005	0.009	0.020	0.040	0.067

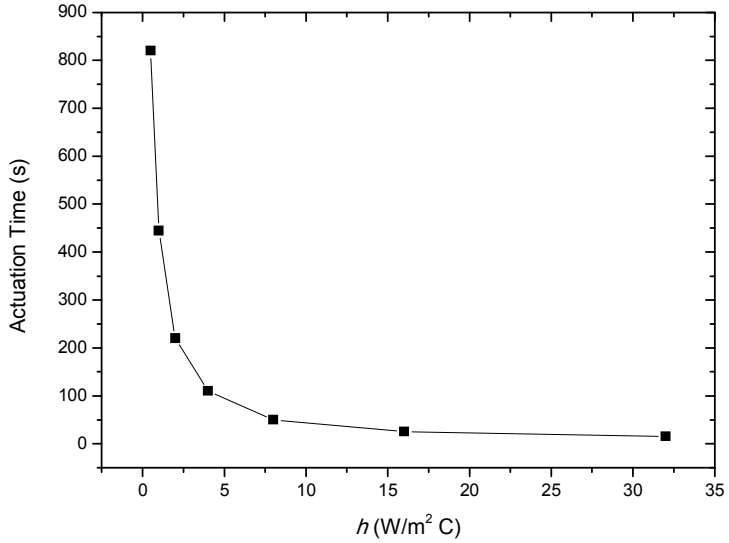

Figure 8. Performance of the SMA device: actuation time as a function of convection coefficient.

Conclusions

This contribution analyses the quasi-static response of shape memory alloy helical springs described by a one-dimensional constitutive model that includes three macroscopic phases in the formulation (two variants of martensite and an austenitic phase). A numerical method based on the operator split technique is employed. An experimental apparatus is developed in order to characterize the thermomechanical behavior of SMA helical springs through load-displacement tests. Numerical results show that the proposed model is in close agreement with experimental data and can be used for the design of actuator using SMA helical springs. It is important to highlight that the hypotheses that phase transformation occurs in a homogeneous way at the SMA wire is realistic providing good results. A performance analysis of the SMA actuator is carried out considering different environmental media represented by convection coefficients. Results indicate that actuation time can be the major drawback of SMA actuators that uses convection as the heat removal mechanisms.

References

[1] K. Tanaka :Journal of Pressure Vessel Technology Vol.112 (1990), pp. 158-163.

[2] M.A. Savi, A.Paiva, A.P. Baêta-Neves and P.M.C.L. Pacheco: Journal of Intelligent Material Systems and Structures Vol. 13 (2002), pp. 261-273.

[3] V. Birman: Applied Mechanics Rev. Vol. 50 (1997), pp. 629-645.

[4] L.G. Machado and M.A. Savi: Brazilian Journal of Medical and Biological Research Vol. 36 (2003), pp. 683-691.

[5] L.G. Machado and M.A Savi: Revista Brasileira de Odontologia Vol. 59 (2002), pp. 302-306

[6] J van Humbeeck: Materials Science and Engineering A. Vol. 275 (1999), pp.134-148.

[7] Z.G. Wang, X.D. Zu, X.D. Feng, S. Zhu, J.W. Bao and L.M. Wang: Materials and Design Vol. 25 (2004), pp. 699-703.

[8] K.K. Denoyer, R. Scott Erwin and R. Ninneman: Acta Astronautica Vol. 47 (2000), pp. 389-397.

[9] L.J. Garner, L.N. Wilson, D.C. Lagoudas and O.K Rediniotis: Smart Materials and Structures Vol. 9 (2001), pp. 673-683.

[10] G. Webb, L. Wilson, D.C. Lagoudas and O. Rediniotis: IAAA Journal Vol. 38 (2000), pp. 325-334.

[11] L.G. Machado, M.A Savi and P.M.C.L Pacheco: International Journal of Solids and Structures Vol. 40 (2003), pp. 5139-5156.

[12] M.M. Khan, D.C. Lagoudas, J.J. Mayes and B.K. Henderson: Journal of Intelligent Material Systems and Structures Vol.15 (2004), pp. 415-441.

[13] A. Spaggiari, I. Spinella and E. Dragoni: Journal of Materials Engineering and Performance Vol. 20 (2011), pp. 489-4961.

[14] S. Min An, J. Ryu, M. Cho and K.J. Cho: Smart Materials and Structures Vol. 21 (2012), pp. 1-16.

[15] I. Spinella and E. Dragoni: Journal of Intelligent Material Systems and Structures Vol. 21 (2010), pp. 185-199.

[16] D.E. Hodgson, M.H. Wu and R.J. Biermann: ASM Handbook Vol. 2 (1992), pp. 887-902.

[17] X.D. Zhang, C.A. Rogers and C. Liang: Smart Structures and Materials Vol. 24 (1991), pp. 79-90.

[18] A. Paiva, M.A Savi, A.M. Braga and P.M.C.L Pacheco: International Journal of Solids and Structures Vol. 42 (2005), pp. 3439-3457.

[19] Y Toi, J.B. Lee and M. Taya: Computer and Structures Vol. 82 (2004), pp. 1685-1693.

[20] M.A Savi and A.M.B. Braga: Journal of the Brazilian Society of Mechanical Sciences and Engineering Vol. 15 (1993), pp. 1-20.

[21] H. Tobushi and K. Tanaka: JSME International Journal Series I - Solid Mechanics Strength of Materials Vol. 34 (1991), pp. 83-89.

[22] A. Paiva and M.A. Savi: Mathematical Problems in Engineering Vol. 2006 (2006), pp.1-30.

[23] L.C.L. Brinson: Journal of Intelligent Material Systems and Structures Vol. 4 (1993), pp. 229-242.

[24] C.M. Jackson, H.J. Wagner and R.J. Wasilewski: NASA-SP-5110 (1972)

[25] P.Y. Manach and D. Favier: Materials Science and Engineering A Vol. 222 (1997), pp. 45-57.

[26] J.E Shigley and C.R Mischke: *Mechanical Engineering Design*, 6th edition, McGraw-Hill, New York, NY(2001).

[27] R.A.A. Aguiar, M.A. Savi and P.M.C.L. Pacheco: Smart Materials and Structures Vol. 19 (2010), pp. 1-9.

[28] M. Ortiz, P.M Pinsky and R.L. Taylor: Computer Methods of Applied Mechanics and Engineering Vol. 39 (1983), pp.137-157.

[29] J. Abadie, N. Chaillet and C. Lexcellent: Journal of Intelligent Material Systems and Structures Vol. 15 (2004), pp.601-609.

[30] J. Abadie, N. Chaillet and C. Lexcellent: Sensors and Actuators Vol. A 99 (2002), pp.297-303.

[31] Y. Luo, T. Takagi, S. Maruyama and M. Yamada: Journal of Intelligent Material Systems and Structures Vol. 11 (2000), pp.503-511.